ELSEVIER

Journal of Nuclear Materials 276 (2000) 289–294

journal of nuclear materials

www.elsevier.nl/locate/jnucmat

Tensile properties and microstructure of martensitic steel DIN 1.4926 after 800 MeV proton irradiation

Y. Dai[a,*], F. Carsughi[b,1], W.F. Sommer[c], G.S. Bauer[a], H. Ullmaier[b]

[a] *Spallation Source Division, Paul Scherrer Institut, CH-5232 Villigen PSI, Switzerland*
[b] *Institut für Festkörperforschung, Forschungszentrum Jülich, 52425 Jülich, Germany*
[c] *APT/TPO, MS H809, Los Alamos National Laboratory, NM 87545, USA*

Abstract

A double-wall window of martensitic steel DIN 1.4926 (11% Cr) was irradiated with 800 MeV protons in the LANSCE facility of the Los Alamos National Laboratory (LANL) to a total number of about 6.3×10^{22} protons (2.8 Ah) in a temperature range from 50°C to 230°C. Tensile tests show that irradiation hardening increases with fluence up to the maximum attained dose of about 6.6 dpa. All irradiated specimens show significant embrittlement, $\leqslant 1.5\%$ uniform elongation and 7.5–9% total elongation as compared to about 11% uniform elongation and 21% total elongation for the unirradiated specimens. SEM observations illustrate that the fracture of specimens changes gradually from ductile mode in unirradiated and low dose specimens to cleavage mode in specimens of high dose ($\geqslant 5.6$ dpa). Intergranular brittle fracture mode has not been observed. Irradiation induced small defect clusters exist in all samples of irradiated material. Both of the size and the density of clusters increase with fluence. At the highest dose of 6.6 dpa large dislocation loops of a size $\geqslant 10$ nm have been observed in addition to the clusters.

1. Introduction

The recent studies on high-power ($\geqslant 1$ MW) spallation neutron sources, e.g., the European Spallation Source (ESS) and the American Spallation Neutron Source (SNS), show that the radiation damage in structural materials of components exposed directly to the proton beam will be a critical issue for the performance and lifetime of such devices [1]. Whereas radiation damage in materials with fission and fusion neutron irradiation has been extensively studied, the effects of spallation type irradiation on materials are not well known. In the absence of intense irradiation facilities, an international collaboration has been setup to investigate spent targets and components from the existing spallation sources. The material investigated in this work is obtained from a beam window of martensitic steel, DIN 1.4926, which was manufactured by the Paul Scherrer Institut (PSI) and irradiated at LANSCE and investigated jointly by PSI, Forschungszentrum Jülich (FZJ) and LANL. Some results on the microstructure in the same materials have been reported in a previous paper [2] showing the amorphisation of precipitates after irradiation. Three-point bending tests and hardness measurements have been carried out at FZJ and the results are reported in Ref. [1]. In the present report the results on tensile properties and radiation induced microstructure will be described.

2. Experimental

The details of the material, the geometry of the beam window and the irradiation experiment were described in Ref. [2]. Only some brief information is given here.

The composition of DIN 1.4926 martensitic steel is: Fe + 0.20C, 0.36Si, 0.46Mn, 0.019P, 0.006S, 10.5Cr, 0.9Mo, 0.64Ni, 0.26V, 0.009W, <0.01Nb, 0.034Cu,

* Corresponding author. Tel.: +41-56 310 4171; fax: +41-56 310 3131.
E-mail address: youg.dai@psi.ch (Y. Dai)
[1] Present address: Facolta di Agrariá, Universitá di Ancona and INFM Unitá di Ricerca di Ancona, 60131 Ancona, Italy.

0022-3115/00/$ - see front matter
PII: S0022-3115(99)00187-7

0.019Co, 0.003Ti in wt%. The material used was normalized at 1050°C for 30 min and tempered at 720°C for 1 h. The beam window was irradiated at LANSCE with 800 MeV protons in the period from July 1989 to October 1990. The real beam time was about 240 days and the total number of protons achieved was about 6.3×10^{22} (2.8 Ah). The irradiation temperature was $\leqslant 230$°C.

As the proton beam position and profile were not perfectly stable for the whole irradiation period, a γ-scan measurement is essentially necessary to detect the beam footprint on the component. The details of this procedure can be found in Ref. [3]. From the data of γ-scan the beam distribution on the window could be fitted with a 2D Gaussian function with σ_x and σ_y of 16.3 ± 0.1 and 23.6 ± 0.1 mm, respectively. From the total number of protons, 6.3×10^{22}, a peak proton fluence of 2.6×10^{25} p/m^2 was obtained, which corresponds to a displacement dose of about 6.8 dpa if a displacement cross-section of 2600 barns is used [4].

The window was cut into strips of 2 mm width for bending tests which employed small bars of $15 \times 2 \times 2$ mm^3 (Fig. 1 (a)). The strip used in this work is about 3.5 mm from the centre line and was exposed to a maximum dose of about 6.6 dpa. A total of six 15 mm long bars were cut from this strip. Calculating the doses from the above proton beam profile yields to 0.3, 1.2, 3.3, 5.6, 6.6 and 5.2 dpa correspondingly. To prepare tensile specimens each small bending bar was cut into three slices, as shown in Fig. 1(a), with a diamond wire saw machine. Then the slices were polished with SiC abrasion papers. The miniature tensile specimens (Fig. 1(b)) were cut from Slice 2 and 3 with the diamond wire saw machine again. TEM samples of about 2×2 mm^2 were cut from the middle area of Slice 1, which corresponds to the gauge area of the tensile specimens.

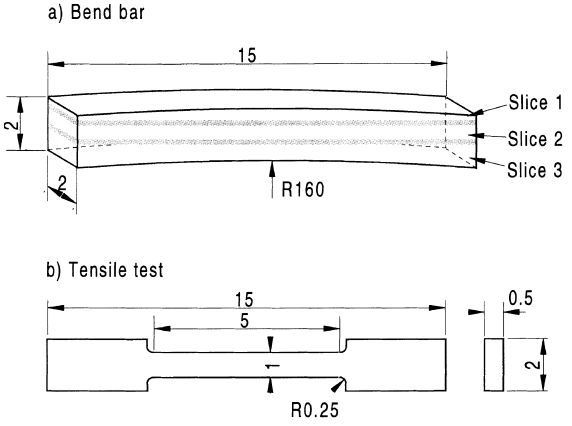

Fig. 1. Sketches showing the geometry of a bend bar and a tensile specimen prepared from the PSI window.

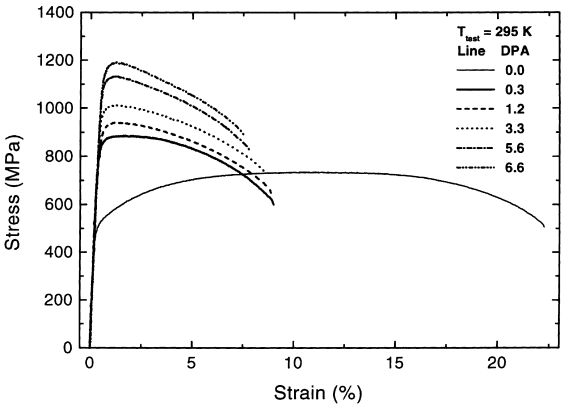

Fig. 2. Engineering tensile curves of both irradiated and unirradiated specimens of DIN 1.4926 martensitic steel tested at 295 K.

Tensile tests were performed on a 2 kN MTS mechanical test machine equipped with a video-extensometer so that the displacement was measured directly from the gauge area. The tests were performed at room temperature (22°C) with a nominal strain rate of 10^{-3}/s (as the machine is soft, the strain rate was smaller at the elastic deformation part). All tensile tests were run to the rupture of the samples. The fracture surfaces were then

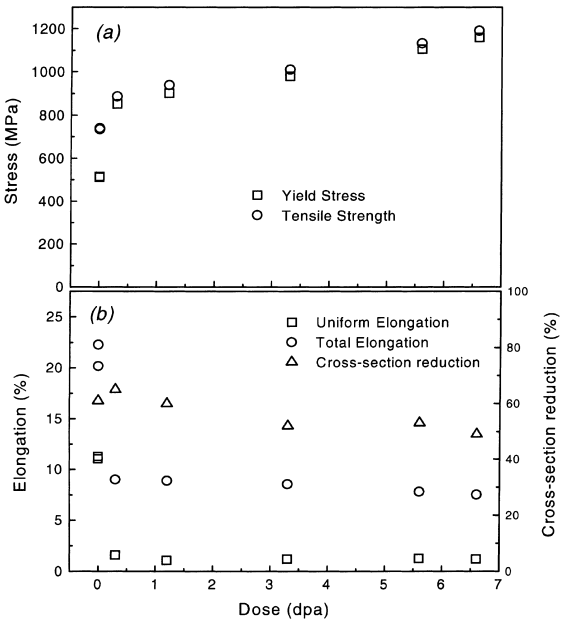

Fig. 3. (a) The upper figure shows the changes in yield stress and ultimate tensile strength and (b) the lower figure shows uniform elongation and total elongation versus irradiation dose of all of tested specimens.

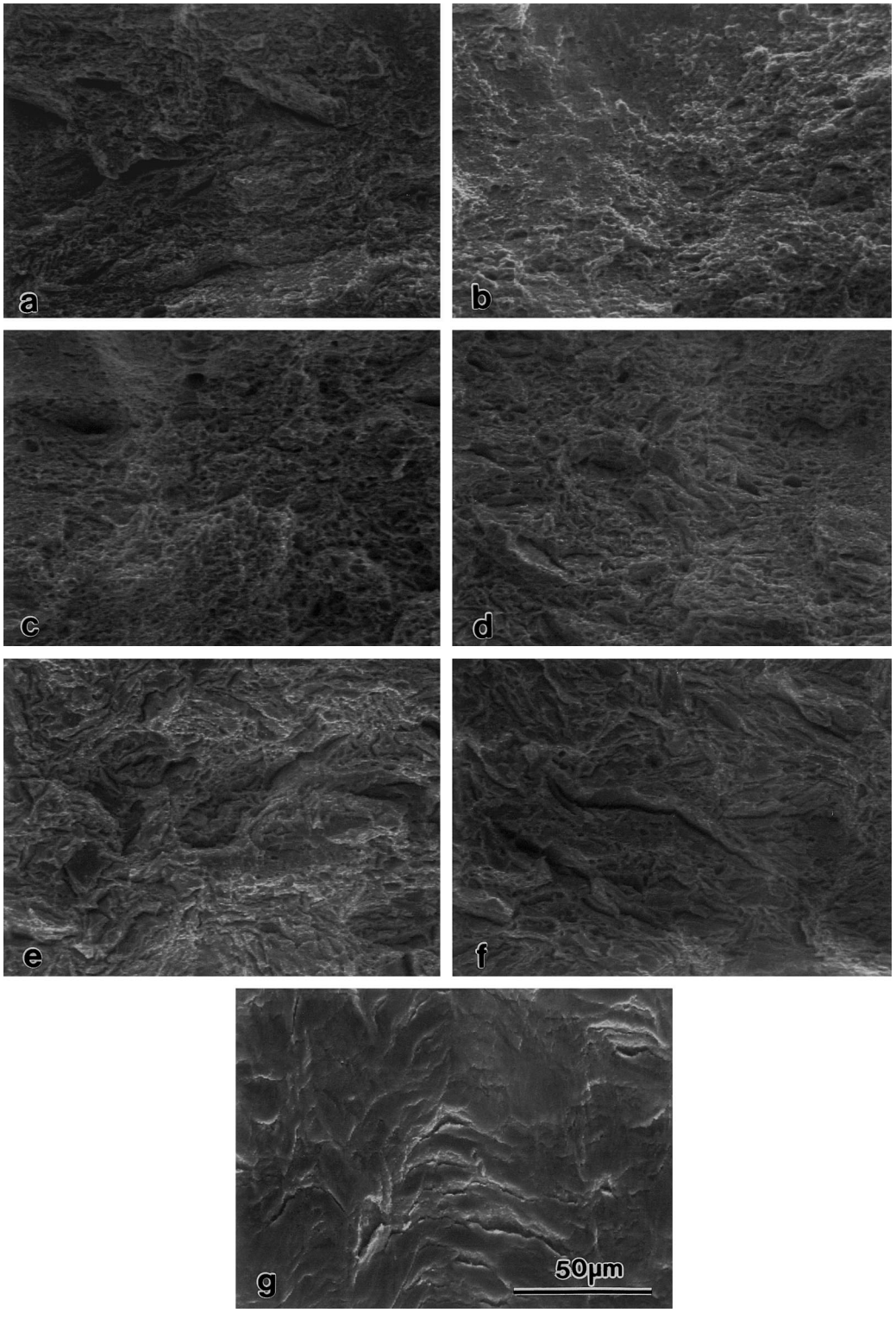

Fig. 4. SEM micrographs show fracture surfaces of specimens (a) unirradiated, (b) of 0.3 dpa, (c) 1.2 dpa, (d) 3.3 dpa, (e) 5.6 dpa, (f) 6.6 dpa and (g) shows micro-cracks on a side surface of a specimen of 3.3 dpa.

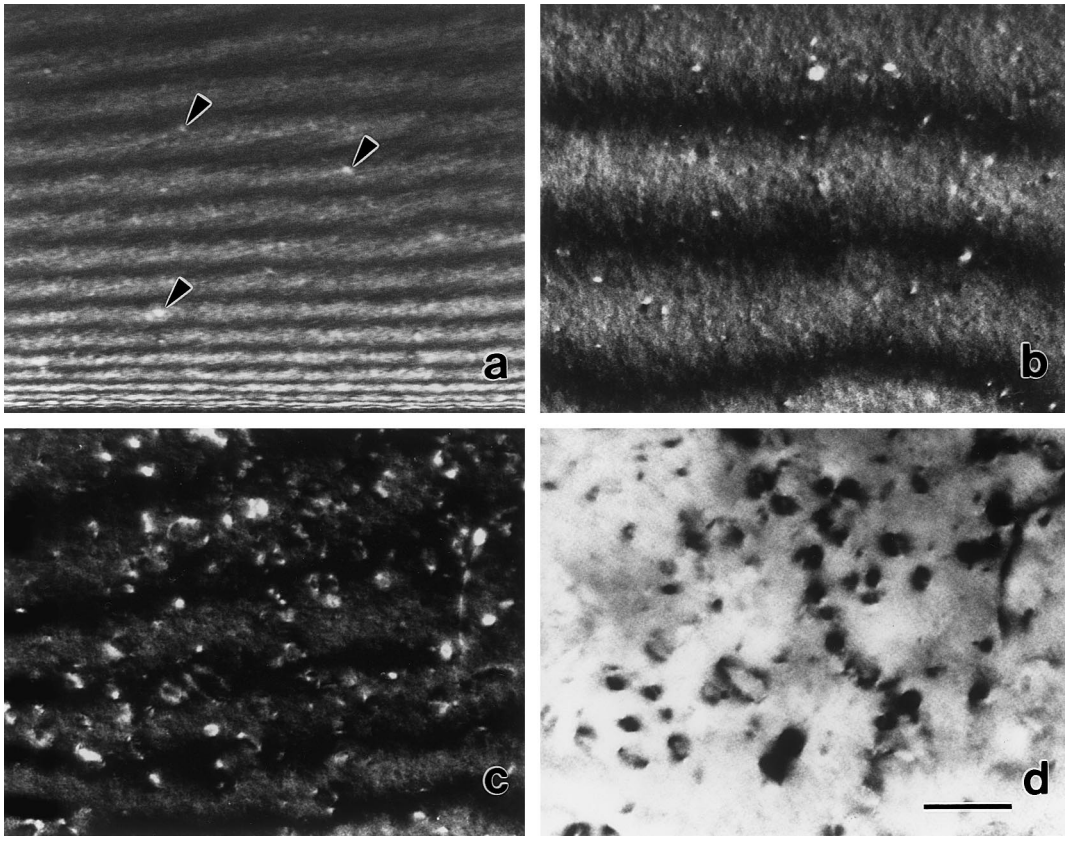

Fig. 5. Micrographs show defect clusters induced by irradiation in specimens of: (a) 0.3 dpa, (b) 3.3 dpa, (c) 6.6 dpa and (d) is the bright field image of (c). The scale in the figure indicates: 35 nm for (a) and 50 nm for (b), (c) and (d).

observed with a scanning electron microscopy (SEM) to identify the fracture mode.

Transmission electron microscopy (TEM) investigation of the microstructure was performed with a JEOL 2010 type microscope equipped with an EDX analysis system. The most often used image conditions were bright field (BF) and weak beam dark field (WBDF) at $(g, 4g)$, $g = 110$.

3. Results

3.1. Tensile properties

The tensile properties were significantly changed after irradiation, even at the low fluence of 0.3 dpa. Fig. 2 shows the engineering tensile stress strain curves of both irradiated and unirradiated specimens. It can be seen that both yield stress and ultimate tensile strength increase with irradiation dose. The uniform elongation decreases drastically after irradiation from about 11% of the unirradiated specimen to less than 1.5% of irradiated specimens. The total elongation reduces to 7.5–9%. Fig. 3(a) and (b) illustrate clearly the changes in the yield stress at 0.2% off-set, the ultimate tensile strength, the uniform elongation and the total elongation versus irradiation dose from all of tested specimens. The cross-section reduction deduced from SEM graphs is also presented in Fig. 3(b), and shows a much smaller change as compared to those of the uniform elongation and the total elongation.

3.2. Fracture mode

Fig. 4 presents part of the fracture surface from unirradiated specimens and irradiated specimens of dose from 0.3 to 6.6 dpa, respectively. It can be seen that the unirradiated specimen (Fig. 4(a)) ruptured in a ductile fracture mode. The irradiated specimen of 0.3 dpa (Fig. 4(b)) shows a similar fracture as the unirradiated specimen. The specimen of 1.2 dpa (Fig. 4(c)) has also a ductile fracture mode in general. A ductile and cleavage mixed mode appears at 3.3 dpa (Fig. 4(d)). At 5.6 and 6.6 dpa (Fig. 4(e) and (f)), the specimens broke in a nearly complete cleavage fracture mode. Therefore, in the present dose range there is a gradual transition from

ductile fracture at low doses to a mode dominated by cleavage fracture at high doses. The observation of side surfaces of specimens reveals that in the area close to the fracture surface micro-cracks were formed at martensite lath boundaries, as illustrated in Fig. 4(g) in irradiated specimen. These micro-cracks are not seen in unirradiated specimens.

3.3. Microstructure

Some results on the microstructure in both irradiated and unirradiated samples have been reported in a previous report [2], showing that precipitates ($M_{23}C_6$) become amorphous and no visible voids or helium bubbles formed after irradiation. Here we present the results on the investigation of the irradiation induced defect cluster structure.

Samples of three doses, 0.3, 3.3 and 6.6 dpa, were observed. Defect clusters produced by irradiation have been observed in all the samples. Fig. 5(a)–(c) are micrographs corresponding to the situations at 0.3, 3.3 and 6.6 dpa taken under WBDF condition (g, $4g$), $g = 110$. In the case of 0.3 dpa (Fig. 5(a)) only very few small clusters are observed. With the dose increasing to 3.3 dpa (Fig. 5(b)) the defect clusters become larger and denser and are easily observed. At high dose of 6.6 dpa (Fig. 5(c)) the defect clusters are very dense and large. There are many large ($\geqslant$ 10nm) loops observed. This can be seen more clearly in Fig. 5(d) which is a BF image of the same area shown in Fig. 5(c).

Defect clusters and small loops were counted and their size was measured from several pictures which were taken under WBDF condition (g, $4g$), $g = 110$ from different areas of each sample. Fig. 6(a)–(c) present the size distribution for each case of the three doses. Two features can be seen from the figures. Firstly, the mean size of the clusters increases with dose from about 3.1 nm at 0.3 dpa to about 5.4 nm at 6.6 dpa. Secondly, large clusters become more and larger with increasing dose. The cluster density has been measured from several areas in each sample and gives $1.3 \times 10^{21}/m^3, 4.2 \times 10^{22}/m^3$ and $1.2 \times 10^{23}/m^3$ corresponding to 0.3, 3.3 and 6.6 dpa. As the thickness of the thin foils was deduced from the number of fringes, the uncertainty of the given densities is estimated to be about $\pm 10\%$.

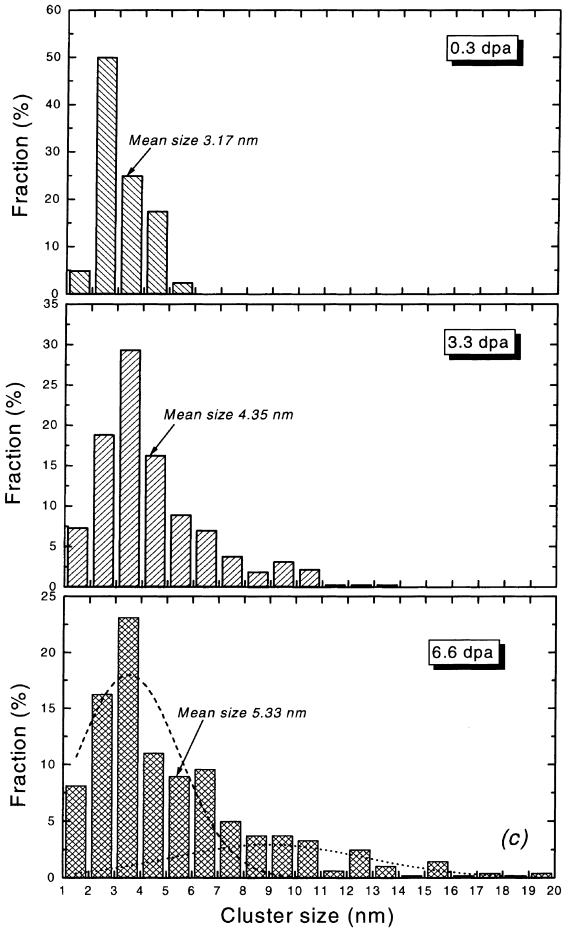

Fig. 6. Defect cluster size distribution in specimens of 0.3, 3.3 and 6.6 dpa.

4. Discussion

The previous hardness and bending tests show that the irradiation hardening increases with dose and has not saturated at the maximum available dose of about 6.8 dpa [1] The present tensile test results agree with the hardness and bending test results. Furthermore, previous tests show the increase of hardness to be proportional to $(\text{dose})^{1/3}$ and the present data, except the one of

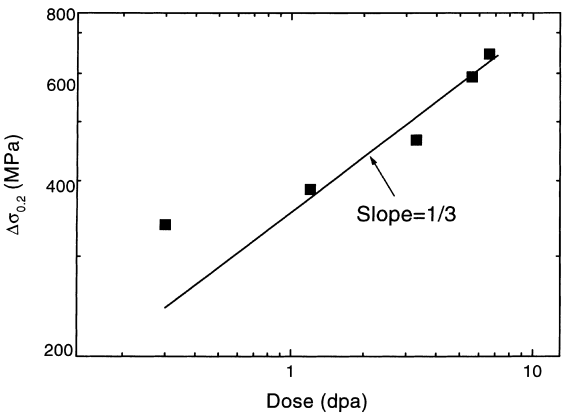

Fig. 7. The irradiation damage induced increase of yield stress as a function of dose.

0.3 dpa, fit this relationship as well, as shown in Fig. 7. The reason for the high increase at 0.3 dpa is probably due to an underestimation of the dose. The position of the sample is relatively far away from the beam center and spallation neutrons should give a considerable contribution to irradiation damage, which has not been taken into account.

The present TEM results agree well with earlier results on martensitic steels irradiated with 590 MeV protons [5], regarding to the defect cluster size and density. In the case of 6.6 dpa the size distribution may be fit by two Gaussian peaks, as shown in Fig. 6(c). The first peak is related to the distribution of small clusters and the second peak gives the distribution of large loops. Such a bimodal size distribution is similar to those observed in austenitic steels irradiated with 800 MeV protons [6] or neutrons [7] at low temperatures ($\leqslant 250$°C). It is believed that the large loops evolved by the accumulation of the small mobile interstitial clusters [8].

The irradiation embrittlement effects in martensitic/ferritic steels at low irradiation temperatures ($\leqslant 300$°C) are well known from neutron irradiation, where they show up as an increase in strength and DBTT and a decrease in ductility and fracture toughness [9,10]. It is clear that the present results show an equivalent behavior in DIN 1.4926 martensitic steel after 800 MeV proton irradiation, namely a yield stress and ultimate tensile strength increase, and a uniform elongation and total elongation decrease. Especially for the uniform elongation, the decrease is serious, from about 11% of unirradiated samples to less than 1.5% after irradiation.

However, tensile results alone may be not sufficient to judge the irradiated material as brittle. Recently Rowcliffe et al. [11] published a comparative study on the tensile and fracture toughness in HT-9 steel at low temperatures ($\leqslant 250$°C). The results show that HT-9 has a very small uniform elongation ($\sim$0.5%) but maintains a high fracture toughness ($\geqslant 250$ Mpa$\sqrt{\text{m}}$) after irradiation at 90°C. The results for the irradiation at 250°C are somehow just reverse: much higher uniform elongation (6–7%) and lower fracture toughness (~ 30 Mpa$\sqrt{\text{m}}$ at test temperature $\leqslant 90$°C and 164 Mpa$\sqrt{\text{m}}$ at 250°C). This means that it is difficult to predict the fracture properties from the tensile results. In the present case, although the uniform elongation is very low the reduction in cross-section is still high ($\geqslant \sim 50\%$) after irradiation (Fig. 3(b)). Furthermore, SEM observations show a cleavage fracture mode at high doses rather than an intergranular brittle fracture mode. Nevertheless more detailed investigations need to be performed in a wider temperature range and also on the fracture properties in order to assess the mechanical behavior of martensitic steels in spallation radiation environments.

5. Conclusions

The tensile properties and microstructure in martensitic steel DIN 1.4926 irradiated with 800 MeV protons at low temperature have been examined. The results show that:

Irradiation hardening increases continuously with fluence up to the maximum attained dose of 6.8 dpa. Irradiation embrittlement effects have been observed. The uniform elongation decreases sharply to $\leqslant 1.5\%$ from about 11% of control samples and the total elongation also reduces by about 60% to a value of 7.5–9%.

Fracture of specimens changes gradually from ductile mode in unirradiated and low dose specimens to cleavage mode in specimens of high dose ($\geqslant$ 5.6dpa). Intergranular brittle fracture mode has not been observed.

Irradiation induced small defect clusters exist in all samples of irradiated material. Both of the size and the density of these clusters increase with fluence. Large dislocation loops of a size $\geqslant 10$ nm have been observed at the high dose of 6.6 dpa, suggesting to a bimodal size distribution of defect agglomerates.

Acknowledgements

The authors would like to thank Mr R. Brütsch (PSI) for his help on SEM observation. The authors are grateful to the staff members of the Hot Cells at PSI, FZJ and LANL.

References

[1] F. Carsughi, H. Conrad, Y. Dai, H. Ullmaier, to be published in Nucl. Technol.
[2] Y. Dai, G.S. Bauer, F. Carsughi, H. Ullmaier, S.A. Maloy, W.F. Sommer, J. Nucl. Mater. 265 (1999) 203.
[3] F. Carsughi, H. Derz, P. Ferguson, G. Pott, W. Sommer, H. Ullmaier, J. Nucl. Mater. 264 (1999) 78.
[4] M. Wechsler, M.H. Barnett, D.J. Dudziak, L.K. Mansur, L.A. Charlton, J.M. Narnes, J.O. Johnson, in: Proceedings of the Symposium on Materials for Spallation Neutron Sources, Feb. 10–12, 1997, Orlando, p. 23.
[5] R. Schäublin, M. Victoria, MRS Symp. Proc. (1999), in press.
[6] J.C. Chen, private communication.
[7] C. Bailat, F. Gröschel, M. Victoria, these Proceedings, p. 283.
[8] M. Victoria, N. Baluc, C. Bailat, Y. Dai, M.I. Luppo, R. Schäublin, B.N. Singh, these Proceedings, p. 114.
[9] R.L. Klueh, K. Ehrlich, F. Abe, J. Nucl. Mater. 191–194 (1992) 116.
[10] F.H. Huang, M.L. Hamilton, J. Nucl. Mater. 187 (1992) 278.
[11] A.F. Rowcliffe, J.P. Robertson, R.L. Klueh, K. Shiba, D.J. Alexander, M.L. Grossbeck, S. Jitsukawa, J. Nucl. Mater. 258–263 (1998) 1275.